Dismantling and remanufacturing strategies in the automotive sector

5 authors, including:

Rico Haase
Fraunhofer Institute for Machine Tools and Forming Technology IWU
31 PUBLICATIONS **86** CITATIONS

SEE PROFILE

Daniele Farioli
Politecnico di Milano
14 PUBLICATIONS **24** CITATIONS

SEE PROFILE

René Selbmann
Fraunhofer Institute for Machine Tools and Forming Technology IWU
12 PUBLICATIONS **64** CITATIONS

SEE PROFILE

Markus Werner
Fraunhofer Institute for Machine Tools and Forming Technology IWU
32 PUBLICATIONS **155** CITATIONS

SEE PROFILE

31st CIRP Conference on Life Cycle Engineering (LCE 2024)

Dismantling and remanufacturing strategies in the automotive sector

Rico Haase[a],*, Daniele Farioli[b], Rene Selbmann[a], Markus Werner[a], Verena Kräusel[a]

a Fraunhofer Institute for Machine Tools and Forming Technology, 09126 Chemnitz, Germany
b Politecnico di Milano, Department of Mechanical Engineering, 20156 Milan, Italy

* Corresponding author. Tel.: +49-371-5397-1375 ; fax: +49-371-5397-61375. *E-mail address:* rico.haase@iwu.fraunhofer.de

Abstract

The contemporary recycling of automobiles takes place on a very baseline material level. In order to fundamentally improve the ecologic footprint of the vehicle, a wider application of remanufacturing strategies is intended. Following different recycling approaches ranging from direct reuse or refurbishment through remanufacturing until repurpose, a well-aimed dismantling followed by manufacturing processes adapted to the post-consumer components is mandatorily required. For use on an industrial scale, environmental efficiency and economic viability must be balanced well. Within the paper, possible remanufacturing technologies and necessary prerequisites such as input data are discussed. For the design of remanufacturing operations, material properties and geometric information are a crucial starting point. Seamless integration of the specific properties is intended to encourage wider utilization of pre-used components and materials. With reference to the well-established process design for metal forming operations, adapted material cards and curvature equivalence values are proposed. The approach is illustrated by a reforming operation, where a brake disc cover is remanufactured from a used car body roof.

Keywords: circular economy, automotive, recycling, dismantling, remanufacturing, secondary raw material, pre-used components

1. Motivation

The ecologic balancing of products and services started with its direct consumptions and emissions. This approach, meanwhile referred to as scope 1, was subsequently extended. Scope 2 covers the indirect emissions of purchased energy during production, while scope 3 even contains the effects adding up along the previous production route of utilized materials and equipment. While the balancing itself can be quite complex [1, 2] and challenging, appropriate countermeasures are obvious. To optimize the environmental footprint, recycling routes must not only be closed, but shortened in order to reduce those scope 3 emissions. Looking at this objective from a product perspective, maximum component value should be maintained. In parallel, the efforts and consumptions of the recycling and manufacturing should be minimized (Fig. 1). This can be categorized as the so called 10R strategies [3].
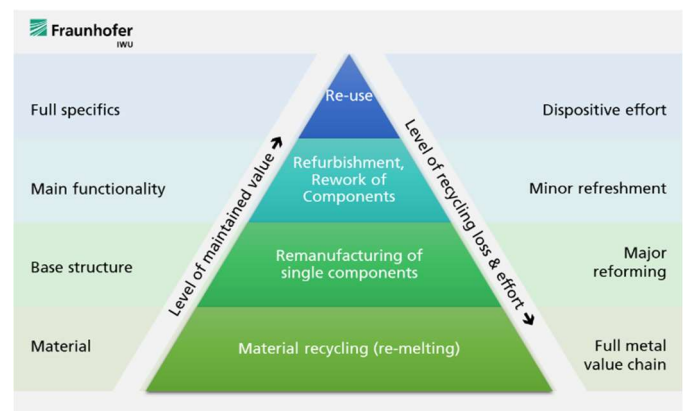

Fig. 1. Value pyramid of maintained value in recycling.

1.1. Challenges

+In the field of automotive manufacturing, sheet metal is the dominant construction material. Even if the amount of secondary raw material in current steel production is 45% [4], recycling takes place on a very baseline material level. Accordingly, the effort for casting, hot and cold rolling, galvanizing and so on counts up (Fig. 2).
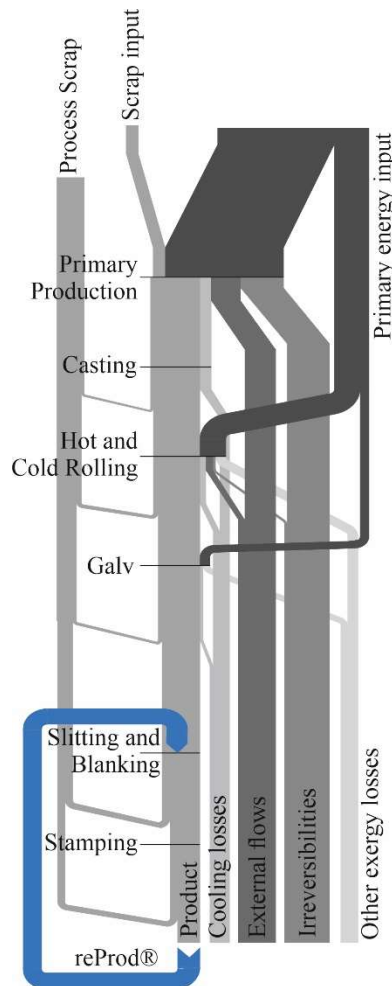

Fig. 2. Conventional recycling loop for metals and reProd® [3].

The aim of shortening the re-entry into the value chain [5, 6, 7] is to be achieved by replacing virgin raw material (coil or blank) by a harvested sheet of pre-used metal. The subsequent process route of sheet metal forming, trimming and joining is highly maturated and well-understood by means of e.g. FEA simulations for conventional, virgin materials. To enable a replacement of the material, a comparable knowledge base about the material properties and technological behavior needs to be developed. This in particular applies to:

- geometric appearance:
  - flatness / curvature and
  - trim contour

- formability:
  - remaining forming limit curve (re-FLC)
  - pre-strain / starting point on material flow curve

1.2. Economic boundary conditions

The solutions towards a lowered product environmental footprint on the one hand need to be technically feasible under industrial conditions. On the other hand, they also need to be economically viable under commercial conditions to make the leap into serial production. From a production engineering perspective, it is state of the art to concatenate primary and subsequent forming operations and continuously monitor the localized material properties. This has been illustrated for a car roof formed into a brake disc cover component. Technically it is feasible, but economically it is far from reasonable. The prerequisite to enable determining the localized material properties of the secondary raw material is a detailed and accurate description of the preceding forming and if applicable flattening operation. This approach is unique for every pre-use scenario and opens up a boundless matrix of variations. As the virgin material still is comparatively cheap, the effortful localized characterization soon sets a limit for potential use cases.

2. Proposed solution

To overcome the discrepancy between ecologically valuable remanufacturing and commercial limitations, a more general approach is proposed. Instead of a specific, localized characterization, a generalized, qualified assumption of material characteristics is utilized to describe the secondary raw material properties in a sufficient manner for a state-of-the-art production process design.

2.1. Methodology

A survey proved that typical car body outer shells feature convex or concave global shapes. For this purpose, the longitudinal and transversal outline of a c-class car (Volkswagen Golf) was elaborated. The transversal curvature is comparatively large with radii about 5000 mm and quite stable along the car body length. In contrast, the longitudinal section varies in a broad range to form the design-specific contour line. Curvature radii usually range from 750 mm to approx. 2500 mm. If one of the curvature radii (r_1, r_2) is very large, this indicates a predominantly bent shape. Most common are convex, double-curved areas in roofs, hoods and fender segments. Some door outer panels show counter-wise orientation of curvatures resulting in a saddle shape. An ancient criterion to describe the relation of those curvatures (k_1, k_2) is the Gaussian curvature (K). It is defined as:

$$K = k_1 * k_2 = \frac{1}{r_1} * \frac{1}{r_2} \tag{1}$$

In contrast to the 3D geometry data, the information about the part's global curvature is compressed to the value of a real number. Still this value contains enough information to compare complex geometries. The trim contour can be defined during the harvesting of the blanks in a manual or automated operation [8]. Car body outer panels are usually formed by a deep or even stretch drawing, with restricted flange draw-in.

Accordingly, material thinning is caused by the surface expansion in deformed versus undeformed (initially flat) state. Drawing processes can be simulated by bulging operations, which are widely used for material characterization purposes. Both, mechanical as well as hydraulic bulging is possible. The latter provides the absence of friction and a good accessibility by visual inspection and measurement. Assuming a uniform strain distribution along a circular section, the elongation ε can be derived from the ratio of curve lengths s in initial condition and l_{curve} in deformed state according to:

$$\varepsilon = \ln\left(\frac{l_{curve}}{s}\right) \tag{2}$$

The length of the curve l_{curve} depends on the bulging height h. It can be calculated as follows:

$$l_{curve} = \frac{\left(\arctan\left(\frac{2h}{s}\right)*4h^2+s^2\right)}{2h} \tag{3}$$

In case of a circular die, the formed bulge is a spherical section. The diameter of the die corresponds to the initial length and is by definition equal all around. Therefore, also the elongation in any section cut is equivalent. By superposition, the equivalent strain is the sum of elongations in two arbitrary perpendicular directions. An equi-biaxial strain is observed.

$$\varepsilon_{eps} = \varepsilon_1 + \varepsilon_2 = 2 * \varepsilon \tag{4}$$

The radius can be calculated from bulge height and diameter according to:

$$r_{curve} = \frac{4h^2+s^2}{8h} \tag{5}$$

In return, the height of a bulge can be derived from the given die diameter and intended radius or curvature respectively.

2.2. Preliminary trials

For an initial feasibility assessment of the flattening operation, small-scale bulge specimen were selected. The considered material was EN-AW-6016 aluminium with a thickness of 1.0 mm. Based on a bulge diameter of 135 mm (Fig. 3, left) and a bulge height of 12 mm, the length of the bulged section equals 137.8 mm (Eq. 2). This corresponds to an engineering strain of 2.1% or a logarithmic strain of 0.021 respectively.
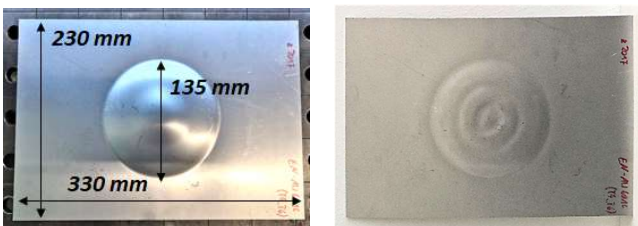

Fig. 3. Specimen with bulged form (left) and flattened shape (right).

The bulging operation was followed by flattening between even plates mounted on a spindle press. The plates blocked towards the sheet metal thickness. The specimen was forced to flat state in clamped position. After opening up the tool, a concentric wave pattern (Fig. 3, right) was observed on the part. The flattened area itself showed only minor local flatness deviation up to 0.3 mm, which is less than half of the sheet metal thickness. In the flange area, a soft, unidirectional bending was observed, lifting the central area approx. 10 mm above the outer rectangular trim line. This result looks promising towards a utilization of flattened secondary raw materials as a replacement for virgin sheet metals.

2.3. Experimental Setup

The small scale of the preliminary trials prevented a reasonable strain measurement. Therefore, a larger model experiment was performed. Aiming for the representation of the manufacturing process on a larger scale, virgin material blanks were processed in a hydraulic maxi-bulge test. The utilized process parameters are summarized in Table 1.

Table 1. Process parameters utilized for hydraulic bulging.

Specification	value	unit
Material grade	DX56D + Z	
Sheet metal thickness	0.7	mm
Specimen size	1000 x 1000	mm²
Bulging pressure	~0.5 (ascending)	MPa
Bulge diameter	500	mm
Bulge height	51.8	mm
Clamping force	15000	kN

For the strain measurement, a rectangular pattern was electro-chemically etched onto the specimen surface. Starting from the initial pattern with 5 mm squares, the intersections were tracked and the corresponding strain was calculated by differentiation of the displacement field. After yielding of the material has begun, the bulge is formed while the fluid pressure increases only slightly. Therefore, the forming of a specific bulge height was not controlled by applying a certain pressure. Instead, volumetric flow was stopped at a triggered height. Thus, dome heights of 52 mm, 12 mm and 6 mm were realized. The corresponding radii can be taken from Table 2.

Table 2. Realized bulge geometries.

	Maxi bulge test		
Diameter s	500 mm		
Dome height h	52 mm	12 mm	6 mm
Curve length l_{curve} (Eq. 3)	514.3 mm	500.8 mm	500.2 mm
Curvature radius r (Eq. 5)	627 mm	2610 mm	5211 mm
Curvature $k = 1/r$	1.595 m⁻¹	0.383 m⁻¹	0.192 m⁻¹
Gaussian curvature $K = k^2$	2.54 m⁻²	0.147 m⁻²	0.037 m⁻²
Elongation	2.86 %	0.15 %	0.04 %
Equivalent plastic strain ε_{eps} (Eq. 4)	0.056	0.003	0.001

The radii achieved in the maxi bulge test correspond very well to the values identified as relevant in the initial survey on automotive outer panels. Still the overall elongation and in particular the equivalent plastic strain (eps) is on a very low level and therefore a challenge for optical measurement. Against this background, the largest deformation was selected for the comparison between calculated values (Table 2) and measurement by the Vialux AutoGrid® system (Fig. 4).
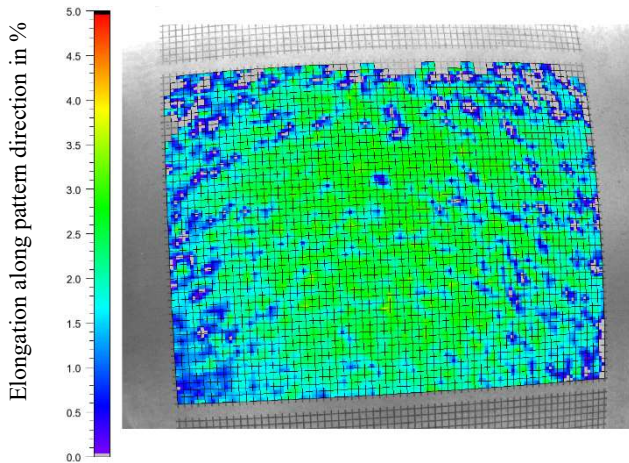

Fig. 4. Elongation measurement by Vialux AutoGrid® system.

Accuracy is severely affected by the precise application of the reference pattern as well as the optic capture of the displacement field after the forming operation. The thinning is calculated by superposition of the elongations in perpendicular directions comparable to the analytic prediction. In this particular case, the directions are defined by the orientation of the pattern on the specimen. Looking at the elongation predicted analytically (Tab. 2) and measured from the trials (Fig. 4), a good compliance can be stated. Fig. 5 shows the superposition of the rectangular elongations resulting in a thickness reduction of about 5%.
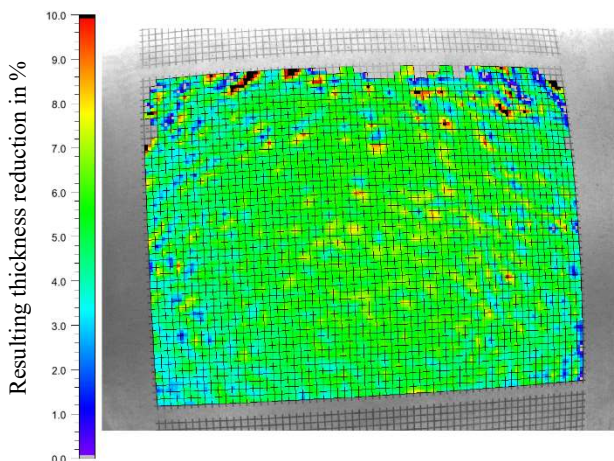

Fig. 5. Thickness reduction by superposition of perpendicular strain.

2.4. Estimation of plastic strain

As discussed in the initial chapter, a reduction in measurement and characterization effort within the remanufacturing route can significantly improve economic efficiency. One central aspect is the reliable prediction of strain in a pre-used component. Therefore, the trial results were analyzed towards potential correlations. The Gaussian curvature (Eq. 1 / Tab. 2) represents the spatial deformation beyond pure bending strain. Assuming predominantly constant radii (r_1, r_2) and thus curvature values (k_1, k_2), the macroscopic shape can be converted into a simple, even scalar equivalent value (K). In the elaborated specimen, it corresponds to the equivalent plastic strain by linear regression (Fig. 6).
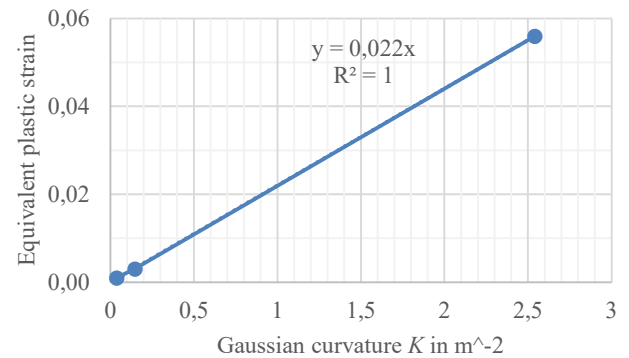

Fig. 6. Correlation of curvature and strain.

2.5. Flattening operation

Due to the large dimension of the preformed specimen, the flattening operation was performed directly between the ram of a hydraulic press and the top surface of a tooling block mounted on the press table. The applied force was 1390 kN, resulting in an average pressure of 1.4 MPa. Comparable to the preliminary trials (Fig. 3), also a concentric wrinkling pattern was observed. Due to the local contact, the actual contact pressure varies significantly. During the closing of the tooling gap, reacting force increases to a maximum. Further, even severe increase in press force actually does not cause any notable change in the strain state. The portion of stored elastic distortion springs back during the opening of the flattening tool. This results in a typical low-curved wave pattern. The height of those imperfections in the flattened secondary raw material blank are compared in Figure 7 and 8.

The overall height of the flattened parts is approximately half of the initial bulge height. In the center area, there is a local strain maximum. Due to the localized contact, surface deformation occurs and leads to this singular strain peak.
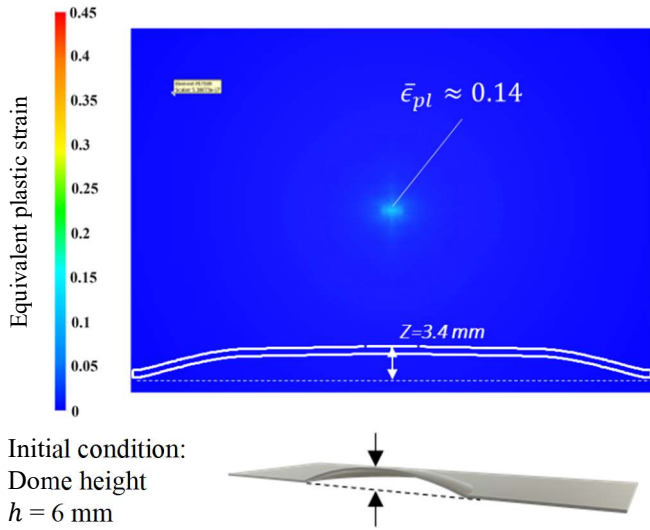

Fig. 7. Flattening of maxi bulge specimen with initially 6 mm dome height: top view on strain distribution and section cut with remaining curvature.
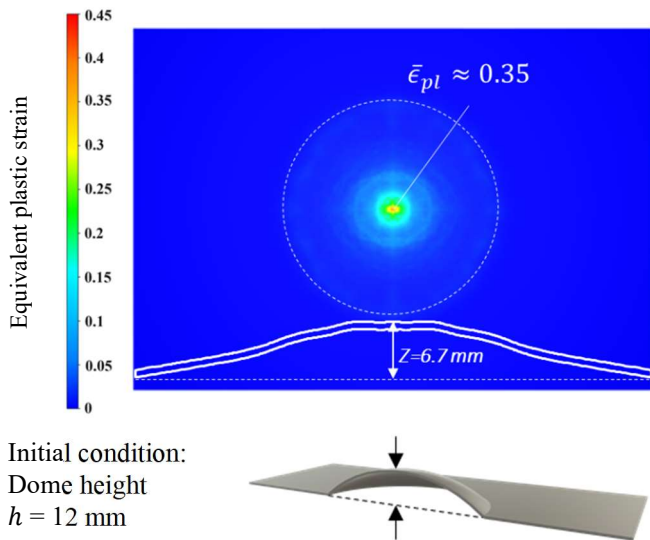

Fig. 8. Flattening of maxi bulge specimen with initially 12 mm dome height: top view on strain distribution and section cut with remaining curvature.

Around this central region, the residuals of the concentric wrinkling pattern still are present on the flattened component. The contact areas are visible as shiny spots on the metallic surface. As radial movement is a restricted boundary condition for the bulged specimen, the flange was removed from a further part. This results in an unrestricted radial movement of the trim edge, limited only by the tangential strain necessary for a lateral displacement. The flattening result of the trimmed bulge is shown in Figure 9.
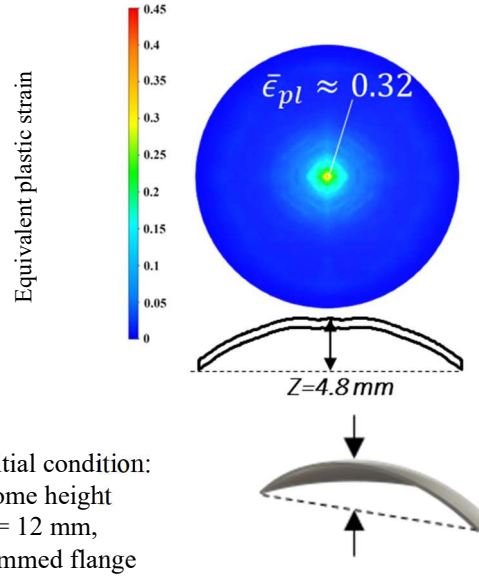

Fig. 9. Flattening of trimmed bulge specimen with init. 12 mm dome height: top view on strain distribution and section cut with remaining curvature.

The remaining height can be reduced from 6.7 mm to 4.8 mm which is a reduction by 28%. The local strain peak at the center remains nearly unaffected.

2.6. Demonstrator part and practical considerations

Regarding potential concerns from the conservative automotive industry, a brake disc cover was chosen for an initial demonstration. This component is present several times on every car, regardless of its size or propulsion system and therefore has a considerable leverage effect. Beside that, typical material grades (HX220YD / HC180B / DC54, depending on car model) and sheet metal thickness of $s_0 = 1,0\ mm$ between the harvested and intended component match each other. The conspicuous reinforcement pattern of the brake disc cover requires a considerable local formability and thus is a suitable indicator for the remaining performance of the SRM.

For practical applications, the flattening operation does not mandatorily require a unique process step. It can be briefly integrated in the subsequent forming operation. As a first example, the flattening of a secondary raw material blank harvested from a car roof was performed during closing the blank holder of the deep drawing stage. Due to the low curvature of the blank, neither proper alignment on the blank holder nor wrinkling was a concern. The tooling equipment and stamped component are illustrated in Figure 10.

The process design was made by a conventional, step-by-step sequence of forming, trimming and re-forming operations in a state of the art AutoForm® FE analysis. Therefore, the full forming history was transferred between the stages. Still the strain portion from the initial forming is several orders of magnitude lower than the subsequent process. This is also congruent to the low equivalent plastic strain values presented in Table 2 and can be considered by an initial offset of plastic strain in the flow curve as well as the forming limit curve (FLC).

drawing die mounted on
hydraulic press

brake disc cover component
with residuals of initial paint

Fig. 10. Combined flattening and deep drawing process of a brake disc cover.

During the initial trials, a circular blank with 424 mm diameter was successfully formed. Still, those parts require a subsequent trimming operation to fulfill the intended functionality. To shorten the process chain and thus even improve the overall economic efficiency, the trimline was predicted by means of Finite Element Analysis (FEA) and directly generated during the cutting of the blanks on a CNC machine "TruPunch5000" as well as in a CNC-controlled laser cutting cell. Ensuring a repeatable positioning in the forming tool, a stable forming operation and stable trim line tolerances could be achieved. For the outer trim, a general trim tolerance of $\pm 1\ mm$ is usual in the automotive industry and met by the parts produced. To date, about a hundred parts have been produced without any disturbing trend or even tool wear.

2.7. Estimation of economic balance

Even though the processing and related cost is strongly depending on the specific geometry of the component, a exemplary calculations can be provided. Aiming for a holistic approach, the conserved energy is compared to the effort during harvesting and further processing of the SRM blank. In the particular case, the weight of the shaped blank is 393 g. Accounting the accumulated energy along the raw material production route [9], this equals an energy amount of 3.75 kWh. The direct consumption of the laser cutting system is 5 kW while in operation. The whole laser processing cell has a peak power consumption of 35.7 kW. The trim length of a single blank is 1326 mm. Based on a maximum feed speed of about 65 mm/s and estimated 25 mm/s in average, the processing time is 53 s. Depending on the handling time (+100% overhead on processing time), the 106 s generate a energy consumption of 1.05 kWh which is less than a third of the conserved value. So, there is still a portion of energy available for the handling and storage process which is not yet included in the balance.

3. Summary and outlook

Heading towards reduced environmental impact of products and resilience in the material supply, utilization of secondary raw materials (SRM) is able to provide a huge leverage effect. Still economic boundaries need to be matched. By a simplified, less effortful assumption of typical SRM properties, an individual material characterization process can be avoided. The ancient Gaussian curvature is a valid tool to compare previous deformation and derive mechanical behavior. By integration of the flattening into the subsequent forming, the economic efficiency of the overall process is improved.

References

[1] Barrow, M., Buckley, B., Caldicott, T., Cumberlege, T., Hsu, J., Kaufman, S., Ramm, K., Rich, D., Temple-Smith, W., "Technical Guidance for Calculating Scope 3 Emissions", https://ghgprotocol.org/sites/default/files/standards/Scope3_Calculation_Guidance_0.pdf, 2013, Accessed: 07.11.2023

[2] Ranganathan, J., Corbier, L., Bhatia, P., Schmitz, S., Gage, P., Oren, K., "The Greenhouse Gas Protocol", https://ghgprotocol.org/sites/default/files/standards/ghg-protocol-revised.pdf, 2004, Accessed: 07.11.2023

[3] Allwood, J.M., "Steel and aluminium in a low carbon future", p. 27-42, ICTP, 2011.

[4] Die Zeit / Statista., "Anteil von Recycling-Material an der Neuproduktion nach Materialart in Deutschland im Jahr 2018", 2018.

[5] Europäische Kommission. (2021). „DELEGIERTE VERORDNUNG (EU) …/… DER KOMMISSION zur Ergänzung der Verordnung (EU) 2020/852 des Europäischen Parlaments und des Rates durch Festlegung des Inhalts und der Darstellung der Informationen, die von Unternehmen, die unter Artikel 19a oder Artikel 29a der Richtlinie 2013/34/EU fallen, in Bezug auf ökologisch nachhaltige Wirtschaftstätigkeiten offenzulegen sind, und durch Festlegung der Methode, anhand deren die Einhaltung dieser Offenlegungspflicht zu gewährleisten ist", EUR-Lex, https://eur-lex.europa.eu/legal-content/DE/TXT/?uri=PI_COM%3AC … … %282021%294987, 2021, Accessed: 07.11.2023

[6] Kräusel, V., „Erschließung von Sekundärhalbzeugen für die material-autarke Produktion", Fraunhofer Institute for Machine Tools and Forming Technology, Chemnitz, 2021.

[7] Werner, M., Haase, R., Hermeling, C., „ reProd® - resource-autarkic production based on secondary semi-finished products", 18th Global Conference on Sustainable Manufacturing (GCSM 2022), Production Technology Center (PTZ), Berlin, 05.-07.10.2022.

[8] Haase, R., „Remanufacturing of metal components: reforming of sheet metal blanks". Webinar CarE-Service Project, 25.05.2021.

[9] Neugebauer, R., „Innovationsallianz Green Carbody Technologies – InnoCaT®". Project Report, 2013.